OPTOELECTRONICS AND ADVANCED MATERIALS – RAPID COMMUNICATIONS Vol. 4, No. 7, July 2010, p. 960 - 964

The investigation of the visible photoluminescence in AlN films deposited by sputtering

DA CHEN*, WEI LI, XU YAN, JINGJING WANG[a], LUYIN ZHANG
Department of Applied Physics, College of science, Shandong University of Science and Technology, Qingdao 266510, P.R. China
[a]*Common Course Department, Shandong University of Science and Technology, Jinan 250031, P. R. China*

We investigate visible photoluminescence properties of the AlN films deposited by sputtering. The influence of defects and impurities in the crystal on the visible emission is presented. The photoluminescence spectra show a broad emission band in the range from 2.2 to 3.3 eV, which consists of two components of the bands centered at 2.5 eV and 3.1 eV. When the native defects reduce and the crystal quality is improved by annealing in nitrogen atmosphere, the shoulder band around 2.5 eV declines. The center of luminescence around 3.1 eV shifts to low energy as the oxygen content increases from 1.1 at. % to 8.5 at. %. The intensity and the center of the emission vary mostly linearly with the oxygen content. Combining the results of X-ray diffraction and X-ray photoelectron spectroscopy, the emission around 3.1 eV can be attributed to the transition from the shallow donor to the deep acceptor related_to the oxygen impurity, while the emission at 2.5 eV may originate from transition from the shallow donor to the deep acceptor related to the native defect.

(Received 05, 2010; accepted July 14, 2010)

Keywords: AlN films, Sputtering, Photoluminescence, X-ray photoelectron spectroscopy

1. Introduction

With the tremendous progress of III-nitrides research in terms of both fundamental understanding as well as devices applications, AlN attracts increasing interest due to the band gap of approximately 6 eV and some excellent properties including high thermal conductivity, good stability at high temperatures, high acoustic velocity and so on. The large range of its excellent properties has made AlN thin film useful in many applications, such as a hard coating[1], electro acoustic devices [2], a buffer layer for epitaxial growth [3], a buried dielectric layer in future silicon-on-insulator devices [4] and Micro /Nano -Electro-Mechanical Systems (MEMS/NEMS) [5, 6]. Recently AlN based deep ultraviolet light-emitting diodes (LEDs) [7, 8] have been reported, which demonstrates the practicability of AlN as an active deep ultraviolet material for future optoelectronic device applications. There have been some reports on the optical properties of AlN films. Near-band-edge luminescence around 6 eV [9-11] and a broad band around 2-5 eV [12-15] from doped and undoped AlN have been observed. Some authors suggested that the luminescence in violet and blue bands may originate from the native defects or oxygen impurity, but little detailed information was given. However, understanding the defect and impurity transitions in AlN is very important for improving the fundamental understanding of material as well as the performance of LEDs, since the presence of strong defect and impurity transitions is detrimental to optoelectronic devices.

In this work we prepared AlN films using radio frequency (RF) sputtering and measure their texture, X-ray photoelectron spectroscopy (XPS) and photoluminescence (PL). XRD rocking curves and photoluminescence spectra have been compared to find out the influence of defects and impurities on the blue photoluminescence band in AlN films. Moreover, the emission mechanism of the blue band is analyzed in detail.

2. Experimental details

The A1N films were deposited using a RF sputtering system (ZKY JGP800). The target was a 4-inch-diameter aluminum with 99.99% purity. The polished 2-inch-diameter (100) Si was used as the substrate. The chamber was evacuated until the base pressure decrease to less than 4×10^{-5} Pa. High-purity argon was then introduced and pre-sputtered the target for 15 min before film deposition. The process parameters were optimized to obtain the strong (002) texture and good quality. The thicknesses of all films were controlled to about 300 nm. The sputtering parameters are summarized in Table 1. In order to investigate the characteristics of the emission band, the samples were annealed in nitrogen atmosphere for 2 h at 600-800 ^{o}C. The ambient pressure kept in 2 Pa during the annealing process. In addition, in order to clarify the effect of the oxygen impurity on the PL properties, a little oxygen with the flows of 0 - 0.3 sccm was induced into the chamber during the deposition process.

Table 1. The sputtering parameters of the AlN films.

Target-to-substrate spacing (cm)	RF Power (W)	Ambit pressure (Pa)	Substrate temperature (°C)	Ar flow (sccm)	N_2 flow (sccm)
5	300	1.2	300	20	10

The crystal texture of the films was identified by X-ray diffraction (XRD, BRUKER-AXS) at wavelength of 0.15418 nm (Cu Kα). The PL spectra was excited by 325 nm line from He-Cd laser (HCL-60B) with 100 mW power, and a double monochromator (Spex 1404) equipped with a charge coupled device detector was employed to analyze the emission light. The stoichiometry of the AlN films were detected by XPS analyses (PHI 5000C) using Al Kα radiation (1486.6 eV). The binding energies of the spectra were referred to that of C 1s peak at 284.5 eV.

3. Results and discussion

Fig. 1 shows the (002) plane X-ray rocking curves of the samples as deposited and annealed in nitrogen atmosphere at 600-800 °C. The inset to this figure shows the XRD pattern of the AlN film as deposited. All samples exhibit a single and sharp (002) diffraction peak around 36°, which indicates preferred (002) orientation. The intensity of the rocking curve is enhanced with the increase of annealing temperature. The full width at half maximum (FWHM) value (0.81°) of the film annealed at 800 °C is observed much smaller than that of untreated one (2.11°), which means that the native defects reduce and the crystal quality is improved after annealing in nitrogen atmosphere at high temperature.

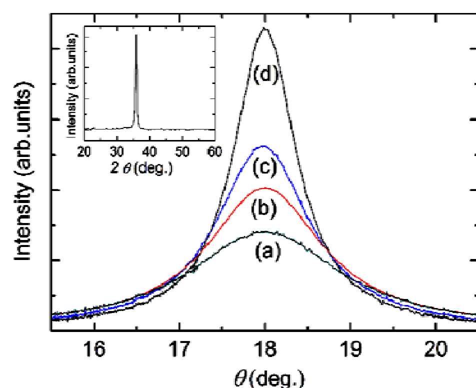

Fig. 1. The X-ray rocking curves of the A1N films as deposited and annealed in nitrogen atmosphere. (a) as-deposited, (b) annealed at 600 °C, (c) annealed at 700 °C, (d) annealed at 800 °C The inset to this figure shows the XRD pattern of the films as deposited.

Fig. 2 shows the room temperature photoluminescence spectra of the the sample as deposited and annealed in nitrogen atmosphere. The excitation light was 325 nm generated by He-Cd laser. A broad emission band is observed in the range from 2.2 to 3.3 eV. The visible band is composed of two peaks which are centered at 2.5 and 3.1 eV. The dashed lines present the two contributions of the luminescence. After annealing at elevated temperature, the shoulder band around 2.5 eV of the untreated sample declines. Combining the PL spectra and the XRD results of the samples, it can be suggested that the emission around 2.5 eV has a strong dependence on the native defects.

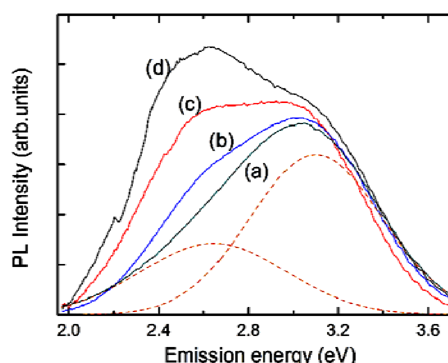

Fig. 2. The room temperature photoluminescence spectra of the A1N films as deposited and annealed in nitrogen atmosphere excited by He-Cd laser. (a) as-deposited, (b) annealed at 600 °C, (c) annealed at 700 °C, (d) annealed at 800 °C. The dashed lines present the two contributions bands of the luminescence.

In order to clarify the origin of the violet emission around 3.1 eV, the stoichiometry of more than 15 samples was surveyed by XPS. Fig. 3 (a) shows a typical XPS survey scan of the film doped with oxygen. The oxygen atomic concentration was controlled by the gas flow in during the deposition process. The carbon signal due to adsorption on the surface was completely removed after the first 50 s sputtering and is not shown. Fig. 3 (b) shows a typical XPS depth profile. There is an initial surface region of high oxygen content, which then drops to a stable level after 100 s sputtering. The average value of this stable level is the atomic concentration we discussed. After an initial surface layer of high oxygen content, the

Al and N+O values tend to stabilize at 50 at. % each, thus, clearly suggesting that the oxygen atoms are substituting for nitrogen in the AlN lattice. The undoped film has the oxygen impurity with the atomic concentration of 1.1 at. % due to the impure deposition atmosphere.

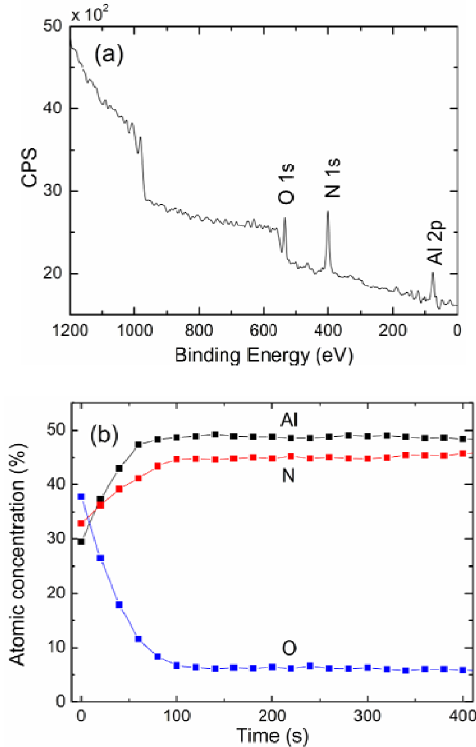

Fig. 3. The XPS spectra of a typical AlN film doped with oxygen. (a) the XPS survey scan, (b) the depth profile.

Fig. 4 shows the rocking curve of the AlN film doped with oxygen content of 8.5 at. %. Although a slightly broadening to 3.36º was observed in the FWHM of the rocking curve compare with that of undoped film, it is considered that the film structure and crystal quality hardly changed in the range of oxygen content.

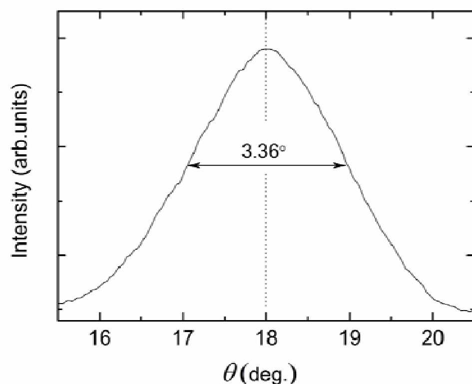

Fig. 4. The (002) plane rocking curve of the AlN film doped with oxygen content of 8.5 at. %.

Fig. 5 shows the typical PL spectra of the samples with the oxygen content from 1.1 at. % to 8.5 at. %. It can be seen that the emission around 3.1 eV shifts to lower energy and obviously gains in the intensity with the increase of oxygen content compared to the peak around 2.5 eV. Fig. 6 shows the dependence of the relative integral intensity and the center of the peak around 3.1 eV on the oxygen atomic concentration. The center of the luminescence shifts from 3.1 eV to about 2.8 eV with the oxygen content increase from 1.1 at. % to 8.5 at. %. The intensity and the center of the violet emission vary mostly linearly with the oxygen content. So it is reasonable that the emission near 3.1 eV can be assigned to oxygen related impurity in AlN crystal.

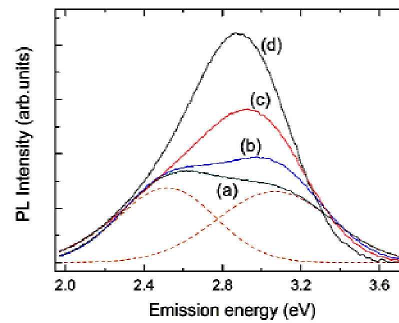

Fig. 5. The room temperature photoluminescence spectra of the typical samples with the oxygen content of (a) 1.1 at. %, (b) 2.8 at. % (c) 5.6 at. % and (d) 8.5 at. %.

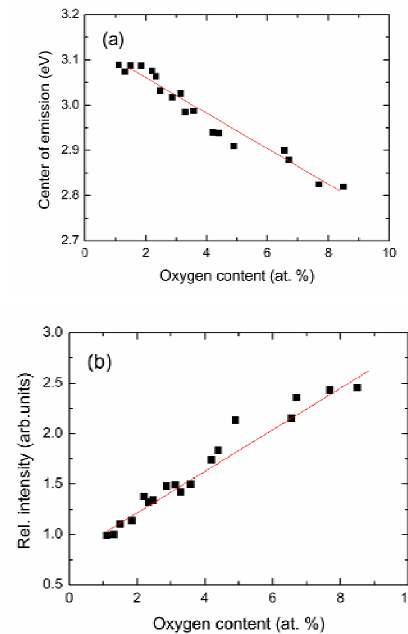

Fig. 6. The dependence of (a) the relative integral intensity ($I_{3.1\ eV}$/ $I_{2.5\ eV}$) and (b) the center of the emission around 3.1 eV on the oxygen atomic concentration.

In the study by Youngman *et al.* [16], a broad band at 2.7 and 3.8 eV from AlN single crystals grown under nitrogen deficient conditions was attributed to the nitrogen vacancy (V_N) but without giving the detailed information. Some groups [17-19] observed the samples with moderate oxygen levels (1-10×10^{19} cm^{-3}) present a broad luminescence band around 4-4.5 eV, which is assigned to donor-acceptor recombination involving oxygen complex. Nam *et al.* [20] though $V_{Al}{}^{3-}$ is the most favorable native defects and accountable for the violet luminescence in AlN with high impurity concentrations. In addition, it is commonly believed that the origin of yellow band in GaN is attributed to isolated cation vacancies (such as $V_{Ga}{}^{2-}$ or $V_{Ga}{}^{3-}$) or impurity related complex (V_{Ga}-complex $)^{2-}$ (such as V_{Ga}–O_N or V_{Ga}–Si_{Ga}) [21]. Similar to the yellow emission in GaN and based on the results shown here, it is believed that the broad luminescence band in AlN films results from the donor-to-acceptor pair transitions between the shallow donor to the two different deep acceptors whose origin is related with the oxygen impurity and the native defect, respectively. In detail, the emission around 3.1 eV can be attributed to the transition from the shallow donor to the deep acceptor related to the oxygen impurity, while the emission around 2.5 eV may originate from transition from the shallow donor to the deep acceptor related to the native defect. Therefore, when the native defects reduce and the crystal quality is improved by annealing in nitrogen atmosphere, the shoulder band around 2.5 eV declines. The intensity and the center of the emission around 3.1 eV also depend on the oxygen content in the AlN films. In addition, the energy separation between the two deep acceptor levels is 0.6 eV, which agrees with the calculated value [14] and has been confirmed by Nam *el al.* [20] in experiment. The redshift of the luminescence at 3.1 eV with increasing of the O content could be related to the enhancement of the $V_{Al}{}^{3-}$ defect with O doping predicted by Stamplf and Van de Walle [22]. Theses results were also observed in the Si doped AlN layers [12].

4. Conclusions

In summary, a broad emission band in the range from 2.2 to 3.3 eV was observed in AlN films deposited by RF sputtering. The band consists of two components of the emission peaks centered at 2.5 eV and 3.1 eV. When the native defects reduce and the crystal quality is improved by annealing in nitrogen atmosphere, the shoulder band around 2.5 eV declines. The center of luminescence around 3.1 eV shifts to low energy as the oxygen content increases from 1.1 at. % to 8.5 at. %. The intensity and the center of the emission vary mostly linearly with the oxygen contamination. Combining the results of XRD and XPS, the emission around 3.1 eV can be attributed to the transition from the shallow donor to the deep acceptor related to the oxygen impurity, while the blue emission around 2.5 eV may originate from transition from the shallow donor to the deep acceptor related to the native defect. The visible luminescence properties of the AlN films suggest that their potential application in photoelectric devices.

Acknowledgments

This work was partially supported by the Research Project of SDUST Spring Bud under Grant No. 2009AZZ056.

References

[1] G. Erkens, R. Cremer, T. Hamoudi, K. D. Bouzakis, I. Mirisidis, S. Hadjiyiannis, G. Skordaris, A. Asimakopoulos, S. Kombogiannis, J. Anastopoulos, K. Efstathiou, Surface and Coatings Technology **177**, 727 (2004).
[2] W. Xu, S. Choi, J. Chae, Applied Physics Letters **96**, 053703 (2010).
[3] Q. Wang, Y. P. Gong, J. F. Zhang, J. Bai, F. Ranalli, T. Wang, Applied Physics Letters **95**, 161904 (2009).
[4] C. Men, Z. Xu, Z. An, P. K. Chu, Q. Wan, X. Xie, C. Lin, Applied Surface Science **199**, 287 (2002).
[5] D. Chen, D. Xu, J. Wang, B. Zhao, Y. Zhang, Vacuum **83**, 282 (2008).
[6] N. Sinha, G. E. Wabiszewski, R. Mahameed, V. V. Felmetsger, S. M. Tanner, R. W. Carpick, G. Piazza, Applied Physics Letters **95**, 053106 (2009).
[7] Y. Taniyasu, M. Kasu, T. Makimoto, Nature **441**, 325 (2006).
[8] T. Toyama, J. Ota, D. Adachi, Y. Niioka, D. H. Lee, H. Okamoto, Journal of Applied Physics **105**, 084512 (2009).
[9] T. Yoshitaka, K. Makoto, M. Toshiki, Applied Physics Letters **90**, 261911 (2007).
[10] G. I. M. Prinz, A. Ladenburger, M. Schirra, M. Feneberg, K. Thonke, R. Sauer, Y. Taniyasu, M. Kasu, T. Makimoto, Journal of Applied Physics **101**, 023511 (2007).
[11] B. N. Pantha, N. Nepal, T. M. A. Tahtamouni, M. L. Nakarmi, J. Li, J. Y. Lin, H. X. Jiang, Applied Physics Letters **91**, 121117 (2007).
[12] E. Monroy, J. Zenneck, G. Cherkashinin, O. Ambacher, M. Hermann, M. Stutzmann, M. Eickhoff, Applied Physics Letters **88**, 071906 (2006).
[13] Y. G. Cao, X. L. Chen, Y. C. Lan, J. Y. Li, Y. P. Xu, T. Xu, Q. L. Liu, J. K. Liang, Journal of Crystal Growth **213**, 198 (2000).
[14] T. Mattila, R. M. Nieminen, Physical Review B **55**, 9571 (1997).
[15] H. T. Chen, X. L. Wu, X. Xiong, W. C. Zhang, L. L. Xu, J. Zhu, P. K. Chu, Journal of Physics D: Applied Physics **41**, 025101 (2008).
[16] R. A. Youngman, J. H. Harris, D. A. Chernoff, Ceramic Transactions **5**, 309 (1989).

[17] J. H. Harris, R. A. Youngman, R. G. Teller, Journal of Materials Research **5**, 1763 (1990).
[18] X. Tang, F. Hossain, K. Wongchotigul, M. G. Spencer, Applied Physics Letters **72**, 1501 (1998).
[19] G. A. Slack, L. J. Schowalter, D. Morelli, J. A. Freitas Journal of Crystal Growth **246**, 287 (2002).
[20] K. B. Nam, M. L. Nakarmi, J. Y. Lin, H. X. Jiang, Applied Physics Letters **86**, 222108 (2005).
[21] D. M. Hofmann, D. Kovalev, G. Steude, B. K. Meyer, A. Hoffmann, L. Eckey, R. Heitz, T. Detchprom, H. Amano, I. Akasaki, Physical Review B **52**, 16702 (1995).
[22] C. Stampfl, C. G. Van de Walle, Physical Review B **65**, 155212 (2002).

*Corresponding author: phychenda@163.com